LONDON'S GLOBAL UNIVERSITY

CENG0037 MSc Research Project

Exploring Pyrite Chemistry in relation to Copper Mineralization in the Delamerian Orogen, South Australia"

by:

Yaojia Sun

Student's registration number: 23030300

Supervisor(s): **Adrienne Brotodewo**

Caroline Tiddy

Travis Batch

A thesis submitted to the University of London for

the degree of Master of Science

Department of Chemical Engineering

University College London (UCL)

September 2023

Declaration

I, Yaojia Sun, confirm that the work presented in this thesis is my own.

Where information has been derived from other sources, I confirm that this has been indicated in the thesis.

Word count: *4041*

Has the written report been submitted on Moodle?

Yes

Have relevant source codes and/or raw data been submitted on Moodle?

Yes

Has the lab space used been cleaned up (if applicable)?

Yes

Yaojia Sun..... 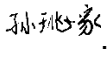 ..... 28 Auguset 2024.....

Student's Name Student's Signature Date

ABSTRACT

This study explores the chemistry of pyrite grains from drilling holes in the Delamerian Orogen, South Australia by MinEx CRC and the Geological Survey. The Scanning Electron Microscopy (SEM) and Inductively Coupled Plasma Time of Flight Mass Spectrometry (ICP-TOF-MS) are used to analyze the morphological and chemical characteristics of pyrite to understand the temperature of formation, different pyrite precipitation events and potential relationship to mineralizing events. Various generations of pyrite are evident in the sample suggesting a complex history with samples potentially linked to both Porphyry Cu-Au and VMS style of mineralization. This highlights the pyrite can be used to provide insight into the conditions of pyrite formation and that this new study area in the Delamerian Orogen shows potential for mineralization and will hopefully lead to further exploration in the region.

TABLE OF CONTENTS

1. INTRODUCTION

Copper is essential to the development of modern industries (Rötzer and Schmidt, 2020). The unique properties, such as malleability, make it highly cost-effective for electrical transmission and it is essential to applications like renewable energy technologies, energy storge and electronic devices (Lawson, 2023). As a result, more copper is required to meet growing global demand. Despite increasing demand for resources, deposits are becoming increasingly harder to find, and the traditional way of mining is challenged by decreasing quantity. Therefore, new innovative ways for exploring are required to find more economic deposits (Pietrzyk and Tora, 2018).

Mineral chemistry is a technique that has recently been developed as certain minerals can be used to find out geochemical signatures that are unique to a particular mineralizing system. Pyrite is one of those minerals that occurs in a range of geological environments (Craig et al.,1998) and can often provide information on the crystallization history of that mineral and any association to a mineralizing system (Liang et al., 2024). Various studies have shown that the chemical zoning of pyrite records fluid-rock interactions during formation and post-crystallization of the mineral (Wu et al., 2019). Additionally, pyrite will typically preserve a range of trave elements (e.g. Co, Ni, As) that are enriched or depleted when associated with different mineral deposits (Cao et al. 2023; Keith et al., 2016). This information can be used to help understand the formation history of pyrite and to determine its potential association with mineralization, which is particularly important for exploration.

This research aims to use pyrite chemistry to increase the understanding of the mineralization potential in the Delamerian Orogen, South Australia, through assessing samples from the recent drilling undertaken by the MinEx CRC and Geological Survey of South Australia. The elemental distribution within pyrite is determined using scanning electron microscope (SEM) and ICP-TOF-MS (Inductively Coupled Plasma Time of Flight Mass Spectrometer) and used to provide insight into the conditions of pyrite formation and its potential association to copper mineralization in the region.

2. BACKGROUND

Pyrite is also known as fool's gold, due to its metallic luster and brass-yellow hue, which often leads to it being mistaken for gold. It is an iron sulfide mineral with the chemical formula FeS_2. Pyrite also has the potential to host numerous trace elements, contain minor amounts of cobalt, nickel, silver and gold in pyrite. (Feick, 2023). This mineral forms in the isometric crystal system with different structure like cubes, octahedrons, pyritohedrons and other combinations. Pyrite is commonly cubic in structure and octahedrons are extremely rare and only exist in Norway's Flat mine (Craig et al., 1998; Feick, 2023). Nowadays, pyrite is mined across around 30 countries worldwide. Annual production is 14 million tons and China accounts for about 85%. (Rickard, 2015)

2.1 Uses of pyrite

Pyrite is an important ore for the production of sulfur and sulfuric acid (Runkel et al. 2009), although today most sulfur is produced from natural gas and petroleum processing (Maslin et al., 2022). However, pyrite is still used in some industrial processes, such as the manufacturing of sulfuric acid and as a source of iron in the production of iron sulfate, which is included in fertilizers, oil refining, and wastewater processing (Liang et al., 2024). As pyrite is a common mineral in different systems, it is also used in geological studies to help understand the physical and chemical environments in which it formed due to the unique textures and chemistry that it preserves.

2.2 Pyrite occurrence in rocks

Pyrite can be formed around the world at many different temperatures and in different geological environments, such as sedimentary, metamorphic, igneous and hydrothermal environments (Schoonen, 2004). Sedimentary rocks consist mainly of shale, sandstone, and limestone, in which pyrite exists in the form of nodules or spreading particles (Craig & Vokes, 2018). Igneous rocks include granite, gabbro and basalt, in which pyrite is formed by cooling crystallization (Kesler et al., 2005). In metamorphic rocks, pyrite is formed under high temperature and pressure. Under these conditions, pyrite is formed when existing pyrite recrystallizes, or other iron-rich minerals change. In hydrothermal environments, pyrite is often formed along with mineralized systems from mineral-rich thermal fluids that move through cracks in rocks (Li et al., 2023).

2.3 Association of pyrite with ore deposits

Pyrite is a common mineral found in many types of deposits. The composition of pyrite is affected by temperature, pH value, fluid interacting with it, and host rock type (Zhang et al., 2024). The composition of pyrite varies with the type of deposit. For example, in porphyry deposits, pyrite often contains high levels of copper and molybdenum due to the influence of magmatic hydrothermal fluids. In volcanogenic massive sulfide (VMS) deposits, pyrite typically shows high zinc, lead, and sulfur content, indicating processes that may be associated with Marine volcanism and submarine hydrothermal systems. (Li et al., 2024).

2.4 Delamerian Orogen case study

The ca. 514-490 Ma Cambrian-Ordovician Delamerian Orogeny was a significant period in Australia's history (Fig. 1). It involved the rifting of the Rodinian supercontinent and the development of a passive continental margin. This phase was followed by the evolution into a convergent margin along the eastern edge of Gondwana, which led to substantial tectonic activity during the Cambrian period. The Delamerian Orogen extends across central and eastern Australia, with length of approximately 2000 km and a width of around 300 km. Remnants of this event is preserved in the South Australian Adelaide Fold Belt, Glenelg River Stavely zones in western Victoria, the Wonaminta Block in western New South Wales and the Precambrian and Cambrian sequences in Tasmania. The Delamerian Orogen comprises a variety of rock types, including those formed during the Neoproterozoic to early Cambrian periods, associated with the Adelaide Rift Complex, and rocks that resulted from subduction

processes along the Gondwanan margin（Gilmore et al., 2023).

The Delamerian basement that extends from the Adelaide fold belt into Victoria and New South Wales in the east is poorly understood as minimal drilling has been undertaken in this area and it us buried by thick layers of sediments in the Murray Basin. However, recent drilling by MinEx CRC and the Geological Survey of South Australia was undertaken in the region in the Quondong Vale and Alawoona drilling areas (Fig. 1).

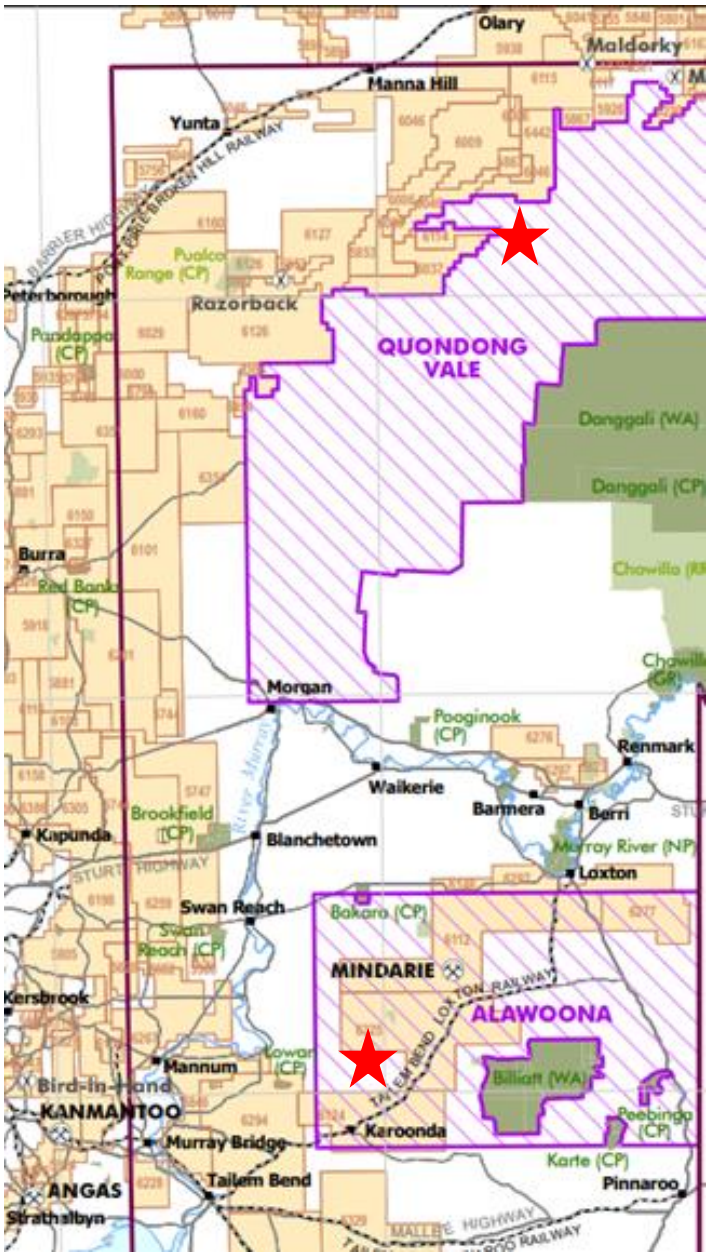

Figure 1: Drill hole Map. Sample locations

2.5 Mineralisation in the Delamerian

The Delamerian Orogen is significant area with potential for mineralization. The Kanmantoo deposit in South Australia could help to gain better understanding of this mineralization. This deposit exhibits significant copper and gold concentrations, which indicates the region's potential for hosting substantial VMS mineralization (Foden et al., 2006). In addition, the Thursday Gossan deposit in western Victoria delivers a good example of porphyry copper-gold mineralization. (Holliday & Cooke, 2007)

3. METHODS

3.1 Sample Preparation

Three drill holes (4331854,4331858,4331859) obtained during the MinEx CRC and Geological Survey of South Australia Delamerian NDI Drilling were sampled in this study (Fig. 1). One sample was collected from each drill hole (total of 3 samples) and selected based on their pyrite grains. Pyrite grains from the samples were mounted in epoxy resin disks, either as individual grains or rock fragments. These mounted samples were ground and polished to analyze textures and collect geochemical data. After that, the samples were subsequently coated with carbon to reduce charging effects during the analysis.

3.2 Scanning Electron Microscopy (SEM)

SEM images of all samples were captured at University of South Australia by Zeiss Merlin FEG SEM and Hitachi Benchtop SEM to identify microstructural characteristics of the pyrite grains, including grain boundaries, inclusions, and growth zones. Hitachi Benchtop SEM, operation parameters include a 10mm working distance, 15 kV accelerating voltage and a range of magnification from x30 to x250. The SEM was operated with a working distance of 10 mm, an accelerating voltage of 20 kV, and a probe current of 3 nA.

3.3 ICP-TOF-MS Analysis

At the Future Industries Institute of University of South Australia, the ICP-TOF-MS was used to trace element chemistry maps of pyrite samples. The ICP-TOF-MS analysis conditions included a repetition rate of 20 Hz, fluence of 3.5 J/cm² and scan speed of 200 µm/s. Calibration was done using standard reference materials NIST610 and KL2-G to ensure accuracy and reliability of the data. Individual spots were 5-10 µm and raw counts per second (cps) images were processed using iolite v4. Pyrite maps for all

elements are in Appendix A.

4. RESULTS

4.1 Pyrite morphology

Representative SEM images showing the morphology of pyrite grains used in this study are shown in Figures 2-4.

Sample 4331854 contains an accumulation of fine-grained pyrite grains that vary between 20-500 µm in size (Fig. 2). The grains shapes vary and are cubic to euhedral and contain a significant number of inclusions at the center.

Sample 4331858 preserves pyrite grains with straight, well-defined grain boundaries that partially display cubic habit typical of pyrite (Fig. 2 c, d). Inclusions are primarily concentrated in the upper half of the grains. Breaks through the grains may be representative of cracks or boundaries between two juxtaposing pyrite grains.

Sample 4331859 displays two different generations of pyrite (Fig. 3). The first generation (Py1) has well defined cubic grains with relatively smooth edges, is largely fractures and has a high degree of inclusions of other minerals. This generation is up to 1 mm in size. The second generation (Py2) are finer grained pyrite and infill areas around Py1 along with other minerals such as chalcopyrite. Py2 has less defined edges and are more porous in texture.

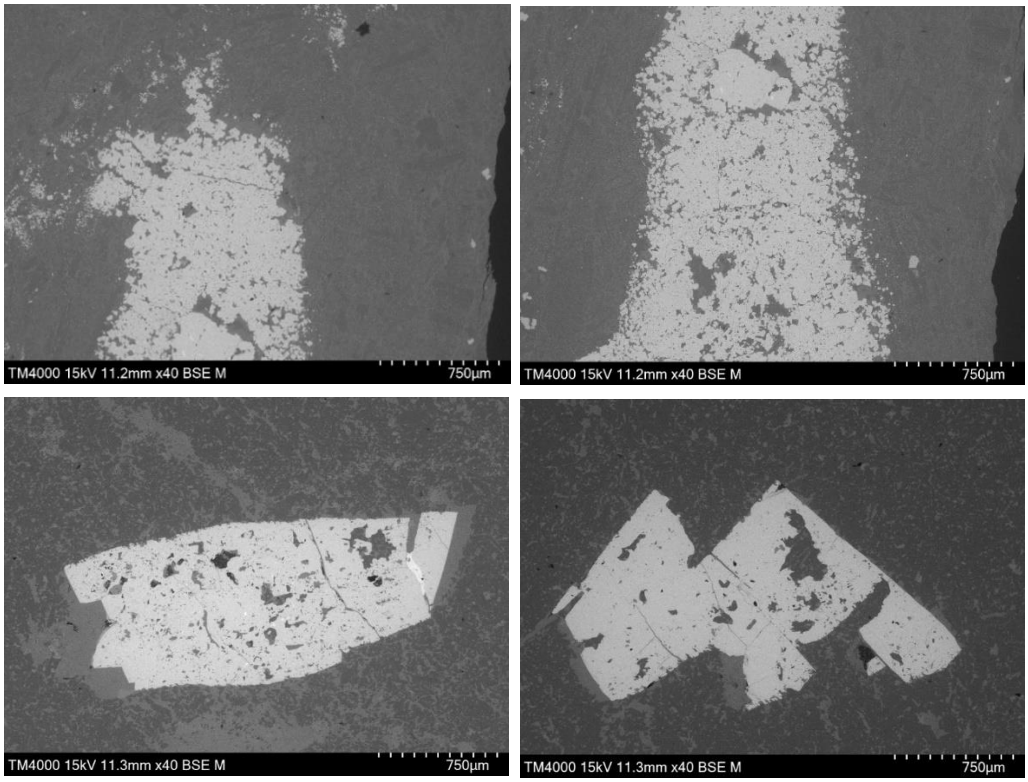

Figure 2: SEM BSE images of sample 4331854 and 4331858. A) sample 4331854 displays an accumulation of fine grained pyrite and fractures present; b) sample 4331854 displays an accumulation of fine grained pyrite and some larger euhedral grains; c) sample 4331858 shows a euhedral grain that is inclusion rich and largely fractured; d) sample 4331858 displays a cubic pyrite grain that was mapped in this study.

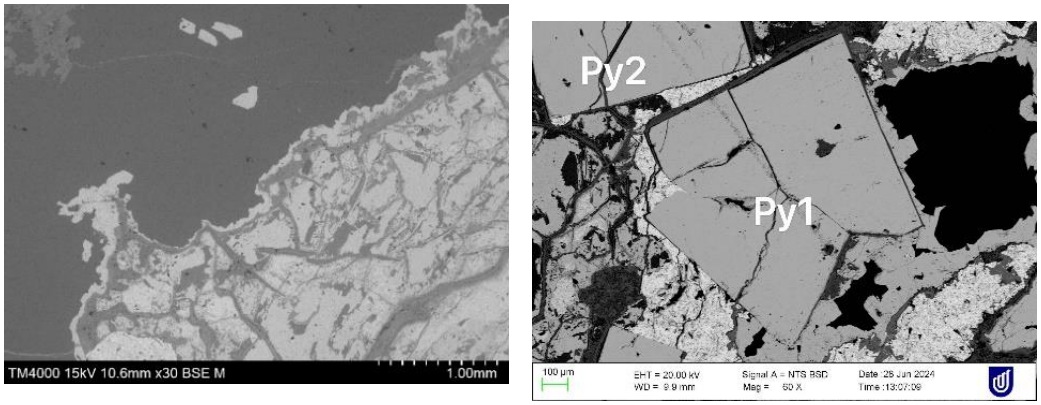

Figure 3: SEM BSE images of sample 4331859. A) displays smaller pyrite grains intergrown with chalcopyrite. These grains are Py2; b) large cubic pyrite grains (Py1) surrounded by finer Py2 grains that infill and are intergrown with chalcopyrite

4.2 ICP-TOF-MS Analysis

Pyrite geochemical maps have been produced for each of the samples on selected grains to show chemical variations across the pyrite grains and different generations.

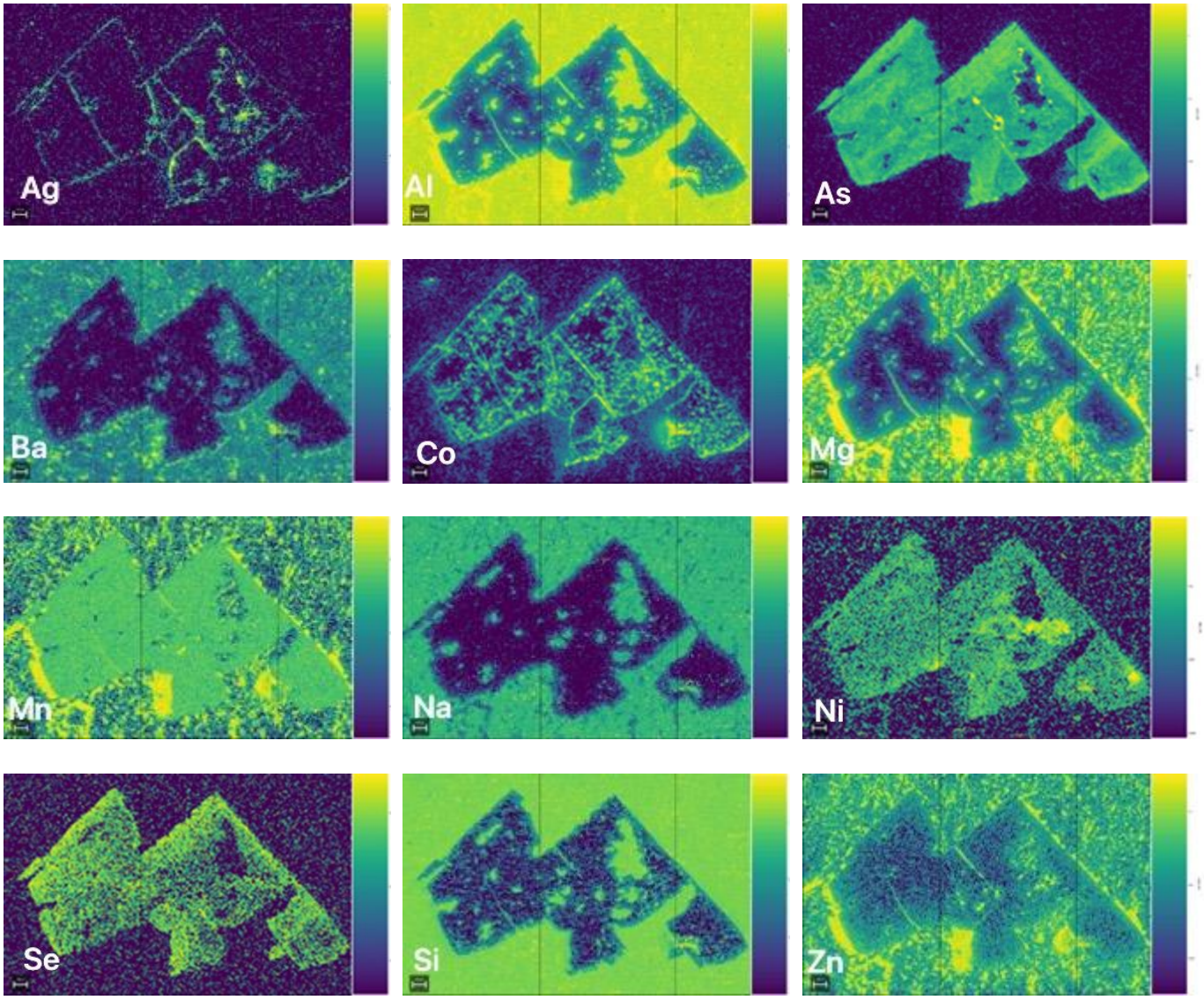

Figure 4. Pyrite maps for sample 4331858.

In Figure 4, the analyzed pyrite sample exhibits a distinct cubic morphology. Elemental mapping shows that the pyrite has moderate concentrations of As, Co, Mn, Ni and Se. The pyrite is depleted in Al, Ba, Mg, Si, and Zn. No clear zoning or latter areas of growth are evident in the pyrite however there is some variability in the Co and Ni content in the grain. Inclusions are present in the grain which are characterized by high concentrations of Al, Ba, Na and Si, with almost no As, Co, or Ni detected. The pyrite grains show some fracturing and Ag is sparsely distributed along these fractures and

along the grain boundaries.

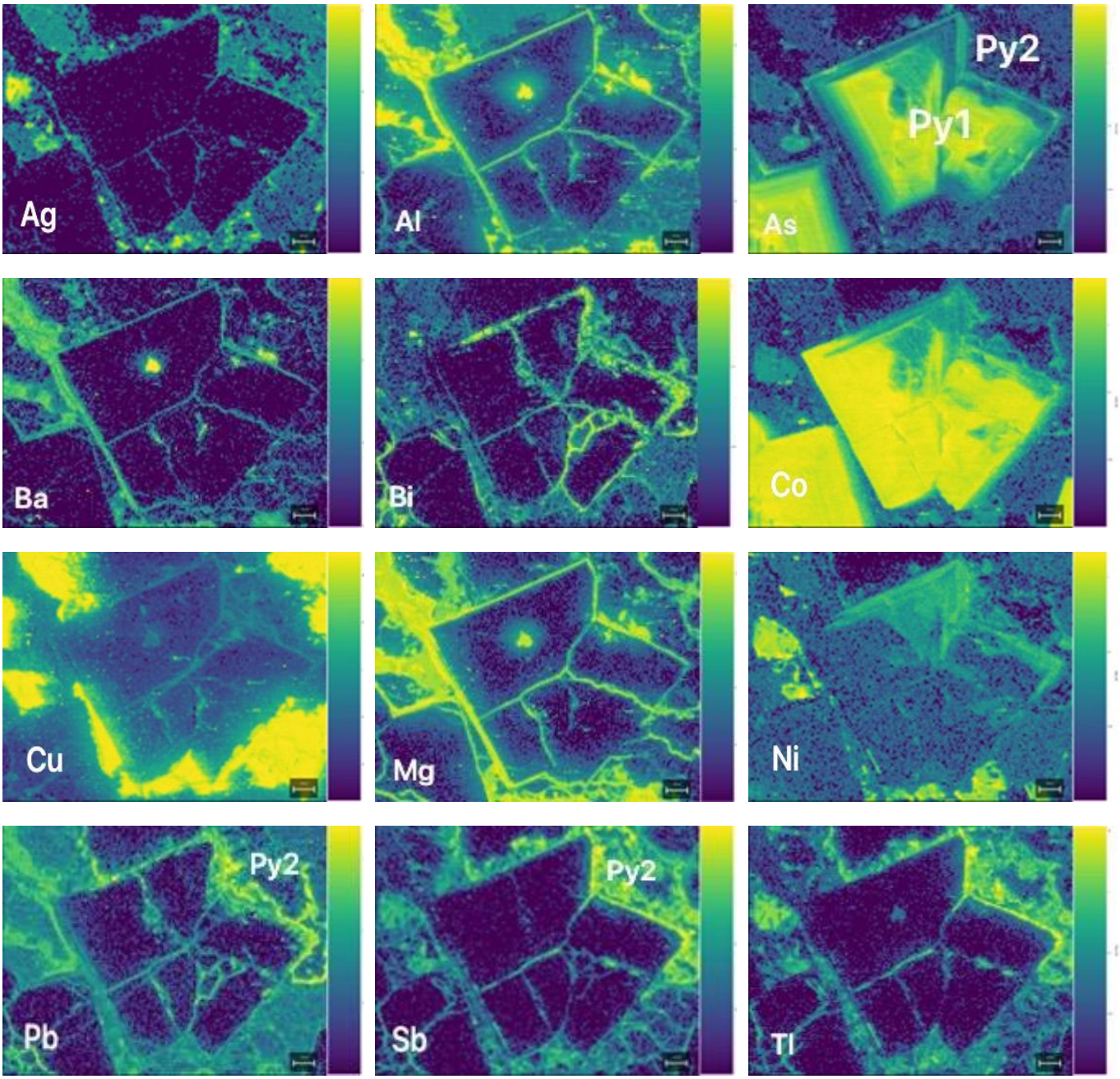

Figure 5: Pyrite maps for sample 4331859 – grain 1

Sample 4331859 is more complicated and shows two generations of pyrite in the elemental map. The first generation of pyrite (Py1) shows a cubic morphology and is highly fractured. Elemental mapping shows that As and Co are enriched in the pyrite, while Ag, Al, Ba, Bi, Cu, Mg, Pb, Sb, and Tl are depleted. Moderate levels of Ni that coincide with lower As and Co values are evident in the upper right zone of this grain,

suggesting that this is a different growth zone in Py1. Zoning is evident within As, Co, and Ni, where As is enriched in the core and depleted around the rims. Fractures are evident in Py1 and are enriched in Mg Pb, Al and Bi suggesting a later fluid would have come through. The second generation of pyrite (Py2) is intergrown around Py1 and appears with chalcopyrite. The chemistry of Py2 is significantly different from Py1. Py2 has moderate levels of Ag, Ni, Ti, Pb, and Sb and is depleted in Al, As, Ba, and Mg.

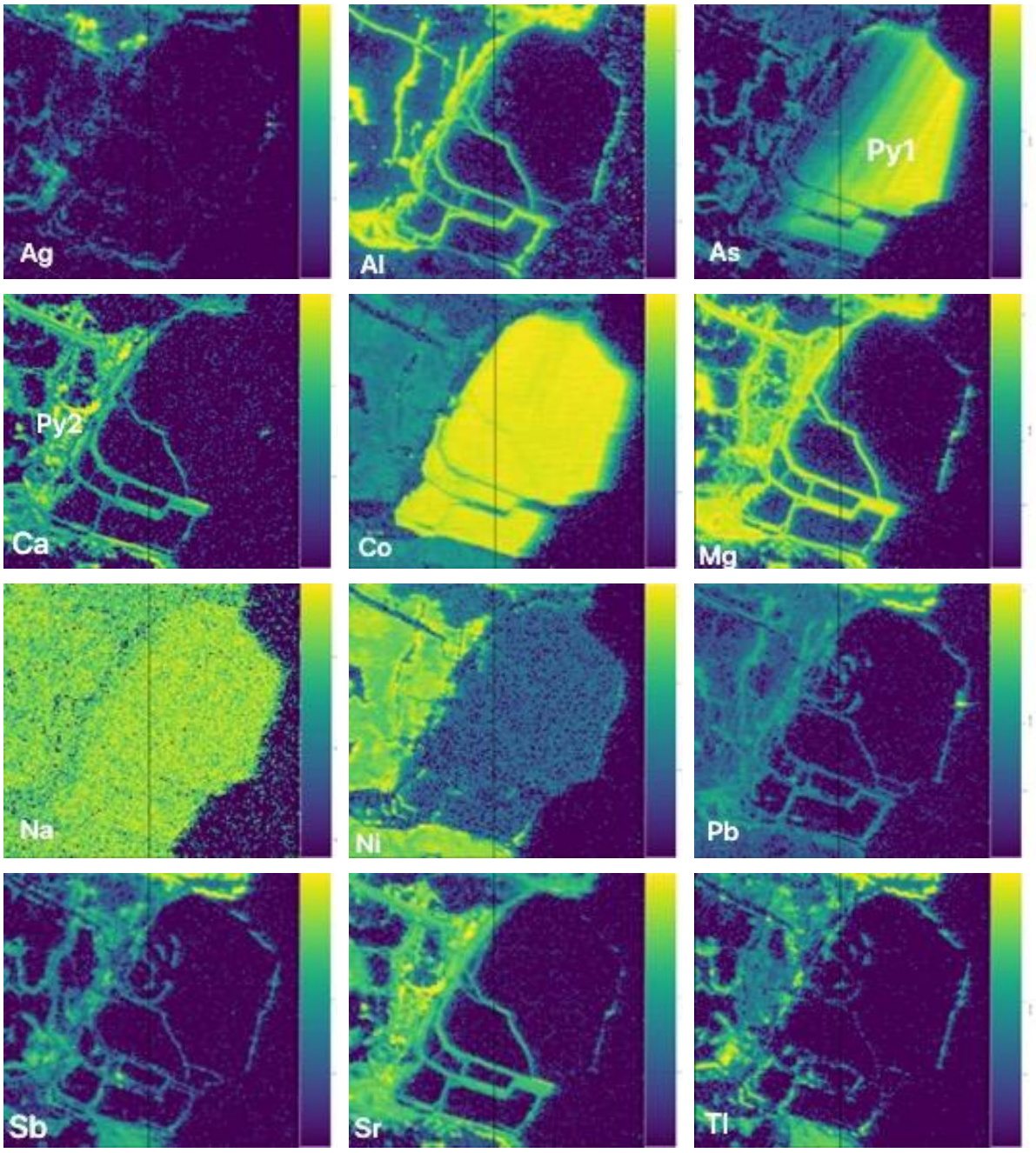

Figure 6: Pyrite maps for sample 4331859 – grain 2

Two generations of pyrite (Py1 and Py2) are also preserved in sample 4331859 (Fig. 6). The coarse grains of Py1 pyrite consist of high As, Co, and Na and are depleted in Ag, Al, Ca, Mg, Pb, Sb, Sr, and Tl. Large fractures cut through this grain and are infilled by a fluid that is enriched in Al, Ca, Mg, and Sr. The concentration of As exhibits zoning and has a decreasing trend from right to left across the mineral. Surrounding Py1 is intergrown chalcopyrite and the second generation of pyrite (Py2). Py2 has moderate to high levels of Ca, Mg, Ni, Pb, Sb, and Sr.

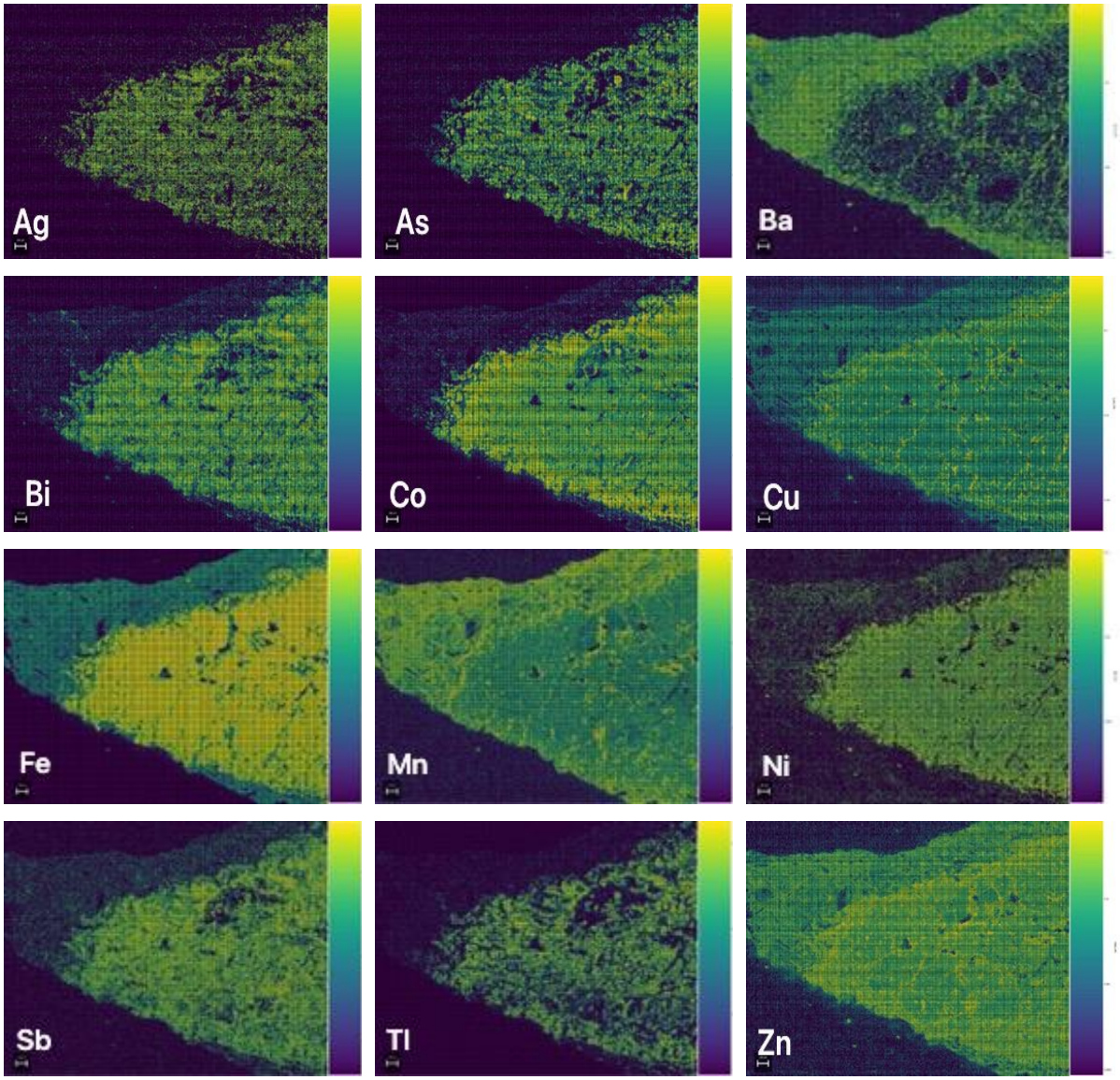

Figure 7: Pyrite maps for sample 4331854

In figure 7, The analyzed pyrite sample shows a distinct two-layer structure, differing from previous samples by having a higher Ag content. In the first layer, Fe is predominant, while in the second layer, elements such as Cu, Mn, Zn, and Ba are more concentrated. Notably, barium is more abundant in the outer layer than in the inner layer. Additionally, Co is more concentrated around the rims, and elements like Cu, Mn, and Zn also show higher concentrations around the rims and follow a fracture pattern within the sample

5. DISCUSSION

Pyrite is a useful mineral that will preserve information on the physical and chemical conditions during the crystallization of that mineral and any post crystallization events that might have affected the region (Gregory et al., 2017). Through the pyrite textures and geochemical maps, a complex history is evident in the Delamerian through the analysis of these samples.

5.1 Pyrite textures

The SEM images and accompanying analyses provide valuable insights into the formation history and post-depositional alterations of the pyrite grains in the studied samples. In sample 4331854, the fine-grained pyrite grains exhibit a range of morphologies from cubic to euhedral, with a significant number of inclusions concentrated at the centers (Fig. 7). The presence of extensive alterations, as suggested by the varied grain shapes and the prevalence of inclusions, indicates that these grains likely experienced significant fluid interactions either during or after their initial formation (Pokrovski et al. 2019). These interactions could have led to the observed morphological changes and the inclusion-rich centers, which are characteristic of late-stage mineralization events or secondary fluid infiltration (Yang et al., 2022).

For sample 4331858, the well-defined cubic habit and straight grain boundaries observed in the pyrite grains suggest a relatively stable formation environment initially. However, the occurrence of fractures indicates post-formational processes. The fractures, likely formed after the initial crystallization, may have served as pathways for later fluid infiltration, introducing new minerals or causing further alterations to the pyrite grains. These features suggest a multiphase history achieved by early pyrite crystallization which was followed by fracturing and subsequent mineralization driven by fluid. Ag is an example which is found to concentrated within fractures as localized enrichment of certain metals (Figure 4)

Sample 4331859 presents a more complex history, with the presence of two distinct generations of pyrite (Py1 and Py2). These two generations differ both texturally and chemically. The first generation (Py1) consists of well-defined cubic grains with smooth edges, but these grains are also highly fractured and contain numerous inclusions. The

fractures in Py1 likely represent post-crystallization events, where subsequent fluids introduced additional minerals,

Py1 is enriched in As and with zoning evident suggesting changing fluid conditions during formation. There are also some areas where it appears to have been reprecipitated by a later fluid as seen with varying As values. The second generation (Py2) of pyrite, characterized by finer grains and more porous textures, clearly formed later, infilling the spaces around Py1 and coexisting with other minerals such as chalcopyrite. The less defined edges and porous nature of Py2 further indicate its formation under different conditions, possibly associated with a separate mineralizing event that occurred after the initial crystallization of Py1. Py2 has moderate Ag, Ti, Pb, Sb and depleted in As and Co relative to Py1. The relationship between Py1 and the formation of Py2 suggests a continued evolution of the mineralization environment, where subsequent fluid activity played a crucial role in the development of the observed textures and mineral assemblages.

Overall, the combination of SEM imagery and the observed inclusion patterns allows us to reconstruct a timeline of mineralization and alteration events, highlighting the importance of fluid interactions in shaping the final morphology of these pyrite grains. The differences between different growth zones, the timing of fractures, and the sequence of mineral deposition could all contribute to gain a more comprehensive understanding of the geological history.

5.2 Conditions of formation

Previous research has established a temperature-based hierarchy for pyrite that allows you to determine the general temperature of pyrite during crystallization based on the elements that are incorporated into the structure (Maslennikov et al. 2009; Steadman et al., 2021). This hierarchy is summarized below and includes some repeating elements which can be incorporated into pyrite at different temperatures (Steadman et al. 2021):

1. High temperature group (>300 ◦C) – Co, Ni, Cu, Se, Te and Bi
2. Mid temperature group (200–300 ◦C) – Zn, As, Sb, and Sn
3. Low temperature group (150–200 ◦C) – Pb, Sb, Ag, Bi, Au, Tl and Mn
4. Seawater group (i.e., diagenetic) – U, V, Mo, and Ni

Based on the incorporation of different elements into pyrite of different generations and within different samples from the Delamerian case study area, we can see that there is a complex history of different events and fluids with different conditions present.

Sample 4331859 provides an insight to take a glimpse of the mineralization process. For Py1, the core of this sample is heavily enriched in high-temperature elements such as Co and Ni, indicating that the initial stage of mineralization occurred at temperatures exceeding 300 °C (Steadman et al., 2021). The different zoning in Py1 suggests that the fluid composition fluctuated during the mineral formation process. These conditions are characteristic of deep-seated hydrothermal systems, where such high temperatures promote the incorporation of these elements into the pyrite structure (Craig et al., 1998). The transition from core to rim in this sample reveals a gradual cooling of the hydrothermal fluids. The outer layers, enriched in Cu, Mn, and Zn, formed under moderate temperatures ranging from 200 to 300 °C. The second generation of pyrite (Py2) shows clear textural and chemical differences to Py1. As Py1 has moderate Ag, Ti, Pb, Sb and depleted in As and Co relative to Py1, it is evident that Py2 likely precipitated from a lower temperature fluid (150-200°C).

Sample 4331854 supports the evidence of lower to mid-temperature mineralization. The elements Zn, As, Sb, and Sn commonly occur in pyrite at medium temperatures between 150 and 300 °C, suggesting that this sample formed as the hydrothermal system began to cool (Steadman et al., 2021) The lack of high-temperature elements in this sample compared to 4331859 suggests that the fluid had already cooled significantly by the time it reached the location where this sample formed.

Sample 4331858 has moderate As, Co, Ni and Mn values (Fig. 4) suggesting it precipitated at a moderate temperature (200–300 ◦C). The lack of Ag and Cu in the pyrite grain suggests that it was unlikely associated with a mineralizing event during precipitation.

In summary, sample 4331859 and 4331858 occur at higher temperatures of 300◦C. Sample 4331854 was derived from moderate temperatures between 200–300 ◦C and sample 4331859 Py2 is derived from lower temperature systems (150-200°C).

5.3 Association with mineralization

The SEM and LA-ICP-MS analyses of the pyrite samples from the Delamerian Orogen give important insights into the mineralization potential in the area. Previous research has used LA-ICP-MS to analyze the mineral chemistry of these pyrite samples from the Delamerian and compared the results to known signatures linked to mineralization (Goeschl et al., 2023; Zhang et al., 2023; Zou et al., 2023). These studies showed that the samples had geochemical signatures that suggest links to porphyry Cu-Au and VMS systems. However, these studies also considered the different textures in each sample, which point

to different origins. Additionally, they did not fully explore whether some samples might not be related to a mineralizing event. By adding pyrite geochemical maps, we can gain further understanding of the origins of these samples and their connection to mineralization.

Sample 4331854 was found to be linked to VMS-style mineralization (Goeschl et al., 2023; Zhang et al., 2023; Zou et al., 2023). VMS systems are usually associated with higher amounts of Tl, W, Mg, V, and Hg in the pyrite structure (Deditius and Reich, 2016; Steadman et al., 2021). The pyrite map from this study shows that elements like Tl, W, and V are part of its structure and that it also formed from a low to mid-temperature fluid. This supports the idea that it is likely connected to VMS-style mineralization.

Sample 4331858 and 4331859 has previously been linked to Porphyry Cu-Au style mineralization (Goeschl et al., 2023; Zhang et al., 2023; Zou et al., 2023) which is commonly associated with high temperature fluids and greater amounts of Co, Ni, Te, Se and lower Tl, Mn, Sb and Hg values compared to lower temperature fluids (Steadman et al., 2021). Sample 4331858 precipitated from more moderate temperature fluids and do not have characteristically high Co, Ni, Te and Se values (Fig. 4 and Appendix A), therefore, it is unlikely that it is linked to a Porphyry Cu-Au mineralizing event like previously interpreted. Sample 4331859 has two different generations of pyrite which was not previously taken into consideration. Py1 has characteristics typical of Porphyry style mineralization due to the enrichment of Co and Ni which suggests it was derived from a higher temperature fluid. This is consistent with previous studies on this sample. The elements present in Py2 are Pb, Sb, Ag, Bi, Au, Tl, and Mn, are indicative of low-temperature environments. These conditions are typical of epithermal systems, where fluids have cooled significantly as they ascend towards the surface. The lower temperatures result in the formation of fine-grained minerals, often concentrated in fractures and other structural features within the host rock (Steadman et al. 2021). Py2 is also intergrown with chalcopyrite which is a common ore mineral in Porphyry Cu-Au systems, therefore this second generation of pyrite may still be linked to porphyry mineralization, but a later time when the fluid cooled.

5.4 Future Work and Limitations

The pyrite maps produced in this study do not have quantitative pixels therefore it is difficult to link this work to exact values from literature however we can still have a good indication on the abundance of different elements samples relative to each other based on the counts per second (CPS) concentrations which is useful for determining links to temperature and trends typically seen in pyrite from different environments. Despite this, we can also use the data from previous studies for quantitative values on these samples (Goeschl et al., 2023; Zhang et al., 2023; Zou et al., 2023).

Future work on sample 4331859 should focus on exploring the implications of the observed secondary pyrite (Py2) formation, particularly its association with chalcopyrite. The presence of chalcopyrite within these samples could be more thoroughly investigated through detailed mineralogical studies, such as or further LA-ICP-MS analysis, to better understand its spatial distribution and formation condition. Additionally, collecting data to determine the timing of these different pyrite growth events would enable us to constrain the timing of the different events and link it to known mineralizing events in the region.

6, CONCLUSIONS

This study has demonstrated the effectiveness of using pyrite chemistry as a tool for understanding mineralization processes within the Delamerian Orogen. The SEM and ICP-TOF-MS analyses have revealed a detailed history of fluid interactions, reflected in the varying morphologies and chemical compositions of the pyrite grains. Sample 4331854 is interpreted to be derived from a low-mid temperature fluid and incorporates elements such as Tl, W and V into its structure, therefore it has been linked to potential VMS style of mineralization. Sample 4331858 does not show typical mineral concertation and temperatures that are associated with Porphyry Cu-Au mineralization likely previously interpreted, therefore it is unlikely to be linked to that style of mineralization. The identification of two distinct generations of pyrite in sample 4331859, with differing elemental enrichments, further suggests that multiple phases of mineralization have taken and that it is likely associated with Porphyry Cu-Au style mineralization. These findings underscore the potential for further exploration in the region, particularly for copper deposits, and highlight the importance of integrating mineral chemistry with geological context in mineral exploration efforts.

7. ACKNOWLEDGMENTS

I am deeply grateful to Dr. Adrienne Brotodewo, Associate Professor Caroline Tiddy, and Travis Batch for their weekly dedication and patient guidance throughout this project. Their insights and encouragement have been instrumental in shaping the direction and quality of this dissertation.

I would also like to express my heartfelt thanks to Susie Ritch and Justin Payne for their invaluable assistance in the lab and with the instruments. Their expertise and support were crucial to the experiment.

8. REFERENCES

Cao, G.S. et al. (2023) *Trace element variations of pyrite in orogenic gold deposits: Constraints from Big Data and machine learning,* Ore Geology Reviews. Available at: https://www.sciencedirect.com/science/article/pii/S0169136823001622 (Accessed: 28 June 2024).

Clark, C., Mumm, A.S. and Grguric, B. (2004) 'Genetic implications of pyrite chemistry from the Palaeoproterozoic Olary Domain and overlying Neoproterozoic Adelaidean sequences, northeastern South Australia', *Ore Geology Reviews*, 25(1-2), pp. 123-134. Available at: https://www.academia.edu/9407616/Genetic_implications_of_pyrite_chemistry_from_the_Palaeoproterozoic_Olary_Domain_and_overlying_Neoproterozoic_Adelaidean_sequences_northeastern_South_Australia (Accessed: 01 July 2024).

Craig, J.R. and Vokes, F.M. (2018) 'The metamorphism of pyrite and pyritic ores: An overview', *Mineralogical Magazine*, 62(6), pp. 873-907. Available at: https://www.cambridge.org/core/journals/mineralogical-magazine/article/abs/metamorphism-of-pyrite-and-pyritic-ores-an-overview/AC0CA0DD274B7444837C359AC0C18A78 (Accessed: 01 July 2024).

Craig, J.R., Vokes, F.M. and Solberg, T.N. (1998) 'Pyrite: Physical and chemical textures', *Mineralium Deposita*, 34(1), pp. 82-101. Available at: https://link.springer.com/article/10.1007/s001260050187 (Accessed: 01 July 2024).

Feick, K. (2023) *Pyrite: Earth Sciences Museum, Earth Sciences Museum | University of Waterloo.* Available at: https://uwaterloo.ca/earth-sciences-museum/resources/detailed-rocks-and-minerals-articles/pyrite#Pyrite%20FeS2%20(Isoclinic) (Accessed: 01 July 2024).

Foden, J. D., Elburg, M. A., Dougherty-Page, J., & Burtt, A. (2006). "The timing and duration of the Delamerian orogeny: Correlation with the Ross Orogen and implications for Gondwana assembly." The Journal of Geology, 114(2), 189-210.

Available at: https://digital.library.adelaide.edu.au/dspace/bitstream/2440/23647/1/hdl_23647.pdf (Accessed: 26 July 2024).

Goeschl, C., Brotodewo, A. and Tiddy, C. (2023) *Linking pyrite chemistry to porphyry and volcanic massive sulfide (VMS) mineralization across the Delamerian Orogeny, South Australia*. Master's Thesis. University College London. (Accessed: 28 August 2024).

Holliday, J.R. and Cooke, D.R. (2007) 'Advances in geological models and exploration methods for copper ± gold porphyry deposits', *Proceedings of Exploration 07: Fifth Decennial International Conference on Mineral Exploration*, pp. 791-809. Available at: https://static1.squarespace.com/static/5f10604a2eb3d3179de51001/t/63f3f8fd2764b604666b18bf/1676933375365/53.pdf (Accessed: 26 July 2024).

Hong, W. et al. (2023) M*etallogenic setting and temporal evolution of porphyry Cu-Mo mineralization and alteration in the Delamerian Orogen, South Australia: Insights from Zircon U-Pb, molybdenite re-os, and in situ White Mica Rb-Sr Geochronology, Economic Geology*. Available at: https://pubs.geoscienceworld.org/segweb/economicgeology/article-abstract/118/6/1291/627839/Metallogenic-Setting-and-Temporal-Evolution-of?redirectedFrom=fulltext (Accessed: 01 July 2024).

Jena, S.S. et al. (2022) *Sustainable use of copper resources: Beneficiation of low-grade copper ores,* MDPI. Available at: https://www.mdpi.com/2075-163X/12/5/545 (Accessed: 28 June 2024).

Keith, M. et al. (2015) *Trace element systematics of pyrite from submarine hydrothermal vents, Ore Geology Reviews*. Available at: https://www.sciencedirect.com/science/article/abs/pii/S0169136815002024 (Accessed: 28 June 2024).

LAWSON, K. (2023) *Conducting change: Why copper is key to a renewable future,* CSIRO. Available at: https://www.csiro.au/en/news/All/Articles/2023/October/Copper-

minerals (Accessed: 28 June 2024).

Liang, C. et al. (2024*) Characteristics, origins, and significance of pyrites in deep-water shales* - science china earth sciences, SpringerLink. Available at: https://link.springer.com/article/10.1007/s11430-022-1200-0 (Accessed: 28 June 2024).

Li H.X. et al. (2024) Geochemical discrimination of pyrite in diverse ore deposit types through statistical analysis and machine learning techniques Research Article Available at: https://pubs.geoscienceworld.org/msa/ammin/article-abstract/109/5/846/638816/Geochemical-discrimination-of-pyrite-in-diverse (Accessed: 01 July 2024).

Limbeck, A. et al. (2015) *Recent advances in quantitative LA-ICP-MS Analysis: Challenges and solutions in the life sciences and Environmental Chemistry - analytical and bioanalytical chemistry, SpringerLink*. Available at: https://link.springer.com/article/10.1007/s00216-015-8858-0 (Accessed: 28 June 2024).

Maslin, M et al. (2022) *Sulfur: A potential resource crisis that could stifle green technology and threaten food security as the world decarbonises,* | Knowledge for policy. Available at: https://knowledge4policy.ec.europa.eu/publication/sulfur-potential-resource-crisis-could-stifle-green-technology-threaten-food-security_en (Accessed: 28 June 2024).

Pokrovski, G.S., Kokha, M.A., Proux, O., Hazemann, J.-L., Bazarkina, E.F., Testemale, D., Escoda, C., Boiron, M.-C., Blanchard, M., Aigouy, T., Gouy, S., de Parseval, P., Thibaut, M. (2019) 'The nature and partitioning of invisible gold in the pyrite-fluid system', Ore Geology Reviews, 109, pp. 545-563. Available at: https://doi.org/10.1016/j.oregeorev.2019.04.024 (Accessed: 26 August 2024).

Pietrzyk, S. and Tora, B. (2018) IOPscience, IOP Conference Series: *Materials Science and Engineering*. Available at: https://iopscience.iop.org/article/10.1088/1757-899X/427/1/012002 (Accessed: 28 June 2024).

Rickard, D. (2015) *Pyrite and the origins of civilization - oxford academic*. Available at: https://academic.oup.com/book/40681/chapter/348374883?login=true (Accessed: 30 June 2024).

Runkel, M. and Sturm, P. (2009) *Pyrite Roasting, an alternative to sulphur burning, Journal of the Southern African Institute of Mining and Metallurgy.* Available at: https://scielo.org.za/scielo.php?script=sci_arttext&pid=S2225-62532009000800007 (Accessed: 28 June 2024).

Rötzer, N. and Schmidt, M. (2020) Historical, current, and future energy demand from global copper production and its impact on climate change, MDPI. Available at: https://www.mdpi.com/2079-9276/9/4/44 (Accessed: 16 August 2024).

Wu, Y.-F. et al. (2019) *Gold, arsenic, and copper zoning in pyrite: A record of fluid chemistry and Growth Kinetics*, Geology. Available at: https://pubs.geoscienceworld.org/gsa/geology/article-abstract/47/7/641/570314/Gold-arsenic-and-copper-zoning-in-pyrite-A-record (Accessed: 28 June 2024).

Yang, Z., Xia, X., Xu, W., Wang, X. & Zhang, Q. (2022) 'Textural and geochemical characteristics of pyrite from the Jinshandian skarn-type iron deposit, central China: Implications for ore-forming processes', *Mineralium Deposita*. Available at: https://doi.org/10.1007/s00126-022-01115-1 (Accessed: 28 June 2024).

Zhang, S. & Brotodewo, A. (2023) *Linking pyrite chemistry to mineralization across the Delamerian Orogeny, South Australia*. Master Thesis. University College of London. (Accessed: 28 June 2024).

Zou, S., Brotodewo, A. & Tiddy, C. (2023) *Linking pyrite chemistry to mineralization across the Delamerian Orogeny, South Australia*. Master Thesis. University College of London. (Accessed: 28 June 2024).

Appednix: